American Mineralogist, Volume 65, pages 670–689, 1980

Petrology of a medium-pressure regional metamorphic terrane, Funeral Mountains, California[1]

THEODORE C. LABOTKA[2]

Division of Geological and Planetary Sciences
California Institute of Technology
Pasadena, California 91125

Abstract

The Funeral Mountains, Death Valley area, California, are a metamorphic terrane characterized by kyanite-bearing assemblages in pelitic schists. Pelitic schists preserve a nearly complete record of the facies types for grades ranging from garnet to sillimanite, and isograds were mapped on the basis of the coexistence of garnet + chlorite, staurolite + biotite, and garnet + biotite + kyanite. Mineral inclusions in garnet provide evidence for the stoichiometry of the reactions chloritoid + quartz = garnet + staurolite + chlorite + H_2O and staurolite + muscovite + quartz = garnet + biotite + kyanite + H_2O. Estimates of the intensive parameters from the distribution of Fe and Mg between garnet and biotite and calcium between garnet and plagioclase indicate that in the high-grade region $P \cong 7200$ to 9600 bars and $T \cong 600°$ to 700°C during metamorphism.

Introduction

The Funeral Mountains consist of a core of metamorphosed sedimentary rocks flanked by relatively unmetamorphosed Paleozoic strata. This metamorphic core comprises a kyanite-bearing terrane, and it has been possible to map Barrovian-type isograds that show a range in metamorphic grade from below garnet zone to sillimanite zone. The metamorphic rocks range in composition, and nearly complete facies types for muscovite-bearing pelitic schists have been preserved.

The geology of the Funeral Mountains and especially the Chloride Cliff and Big Dune 15′ Quadrangles is being mapped by B. W. Troxel and L. A. Wright, who kindly provided a copy of the preliminary map. The geology of the southern part of the Funeral Mountains is described by McAllister (1974), and the geology of the Grapevine Mountains which are contiguous with the Funeral Mountains to the north is outlined by Reynolds (1974) (Fig. 1). The Grapevine–Funeral Mountains chain comprises late Precambrian, Paleozoic, and Tertiary sedimentary, metasedimentary, and volcanic rocks.

The oldest rocks are a sequence of interbedded pelitic schist, calcite marble, micaceous quartzite, and amphibolite. Pelitic schist comprises about half of this section and is prominent in the lower and upper part. Micaceous quartzite, calcareous quartzite, and marble make up the middle part. The occurrence of amphibolite in the lower part and conglomerate in the upper part led to the correlation of these rocks to the Pahrump Group (Troxel and Wright, 1968). The lithologies in this section are not directly correlative to the formations which compose the Pahrump Group elsewhere in the Death Valley area.

The Pahrump Group is overlain by the Johnnie Formation which consists predominantly of pelitic schist and quartzite. The Stirling Quartzite overlies the Johnnie Formation and consists of quartzite, micaceous quartzite, and minor carbonate layers. Pelitic layers occur near the base of the Stirling Quartzite. In the Chloride Cliff Quadrangle, the Stirling Quartzite is locally overlain by argillite and quartzite of the Wood Canyon Formation. This Paleozoic section is overlain by middle and upper Tertiary fluvial, lacustrine, and volcanic rocks. The generalized geology of the Chloride Cliff Quadrangle, which encompasses the majority of the metamorphic rocks, is shown in Figure 1.

The structure of the Funeral Mountains is domi-

[1]Contribution Number 3338.

[2]Present address: Department of Earth and Space Sciences, State University of New York at Stony Brook, Stony Brook, New York 11794.

0003–004X/80/0708–0670$02.00

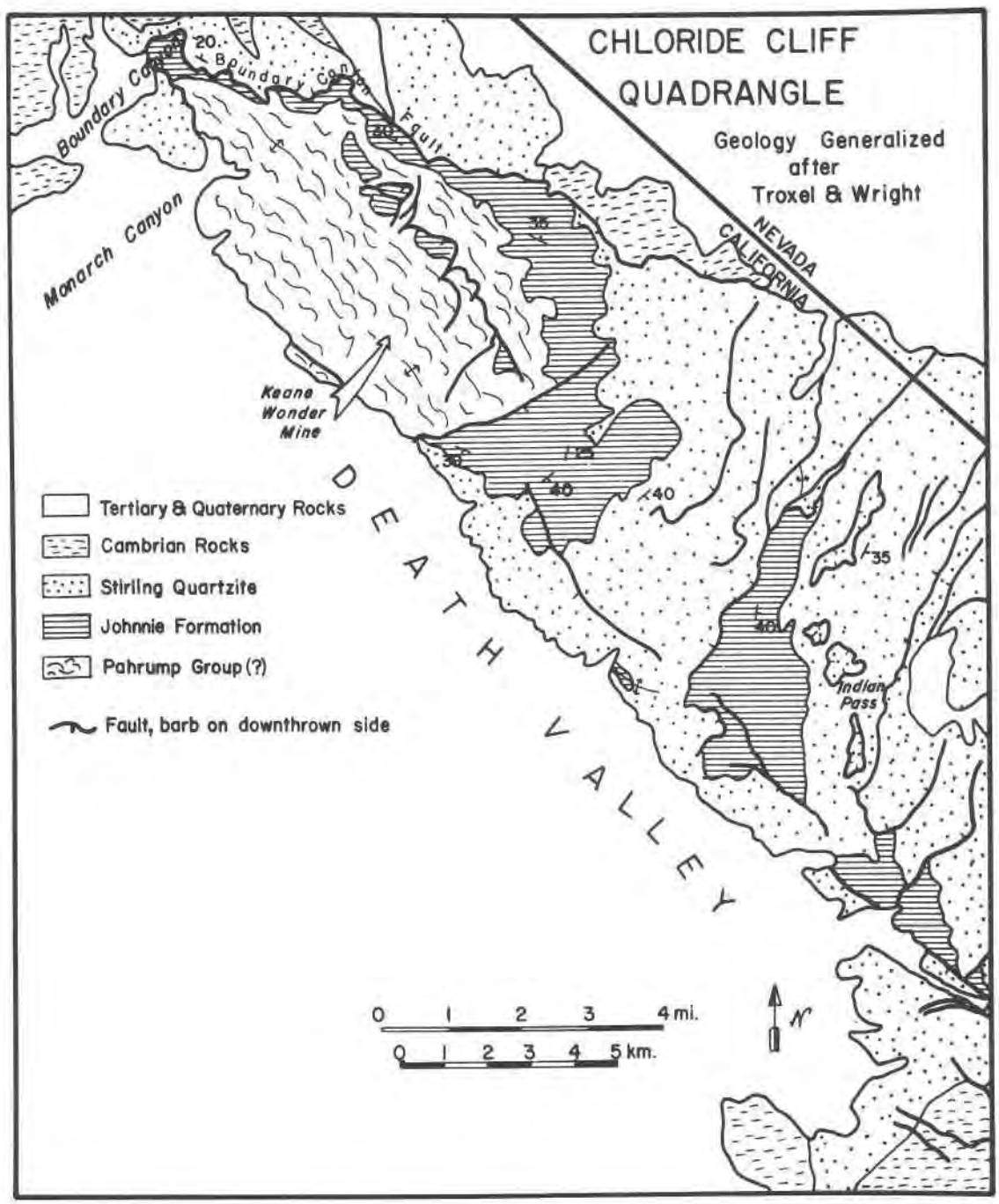

Fig. 1. Generalized geology of the Funeral Mountains, Death Valley, California. The northern Funeral Mountains comprise late Precambrian and Cambrian sedimentary and metasedimentary rocks which are folded into a northwest-trending, doubly plunging anticline and which are cut by shallow-dipping, normal faults. The geology of the Chloride Cliff Quadrangle is modified from the preliminary geologic map by Troxel and Wright (personal communication).

nated by a doubly-plunging anticline that culminates in the high-grade metamorphic terrane near Chloride Cliff. The high-grade metamorphic rocks in this "core" are separated from low-grade metasedimentary rocks by a major fault, here called the Boundary Canyon fault, which has a gently undulating surface and dips generally north. Similar gently north-dipping faults also displace the folded metamorphic ter-

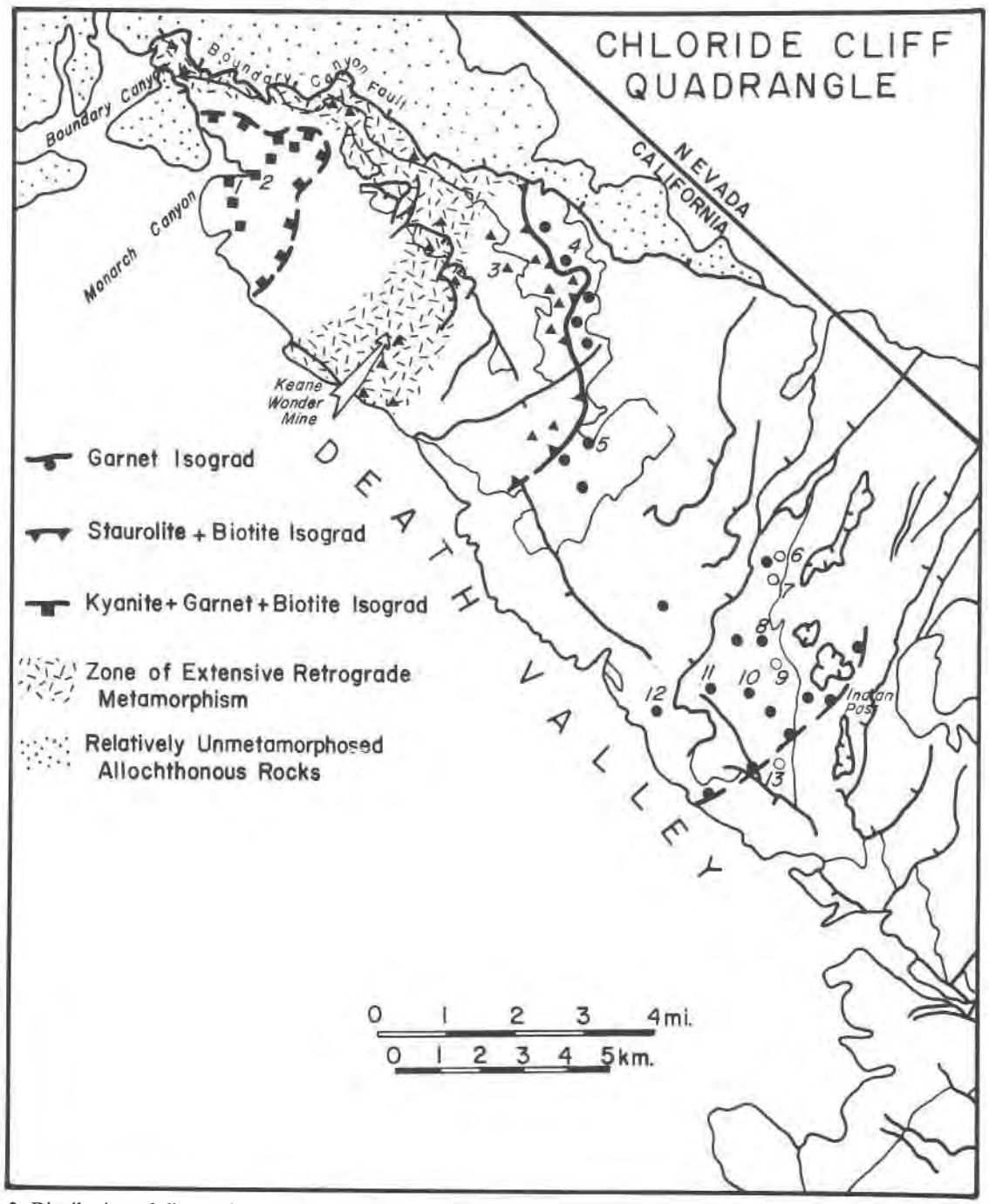

Fig. 2. Distribution of diagnostic assemblages, metamorphic isograds, and localities of analyzed samples. Filled circles represent garnet + chlorite assemblages; triangles represent staurolite + biotite assemblages; squares represent kyanite + garnet + biotite assemblages. Numbers indicate analyzed samples and are listed in Table 1. Open circles are localities of analyzed samples that contain other assemblages.

rane. Rocks as young as Oligocene are displaced by these faults and Pliocene strata on the upper plate of the Boundary Canyon fault are warped (Wright and Troxel, personal communication).

Two foliation surfaces are well developed in the metamorphic rocks. The older consists of a schistosity that is defined by the parallel alignment of muscovite and biotite grains and is oriented parallel to

the compositional layering. A second foliation developed after the growth of porphyroblasts and consists of microfolds ("strain–slip" cleavage) whose axial planes lie at a high angle to the bedding.

The metamorphic isograds mapped in the Funeral Mountains are delineated on Figure 2. Metamorphic grade increases from southeast to northwest, and isograds are cut off by the Boundary Canyon fault. The isograds do cut across the stratigraphy, but, in general, metamorphic grade increases with stratigraphic depth. The highest-grade rocks occur in Monarch Canyon, near the culmination of the anticline, where sillimanite-bearing assemblages occur. Migmatites occur in the canyon bottom, and these high-grade rocks are intruded by minor bodies of leucocratic, muscovite-bearing granitic rock.

Extensive retrograde metamorphism has affected the high-grade rocks in the Keene Wonder Mine area, Chloride Cliff, and along the Boundary Canyon Fault, where most of the mafic minerals are altered to chlorite. The retrograded area corresponds to a mineralized area which was heavily prospected for gold in the early 1900's, and to the post-metamorphic tectonic dislocation.

The age of metamorphism is not well constrained. Metamorphism occurred after the deposition of the affected strata and before the development of the Tertiary Boundary Canyon fault. Muscovite from a pegmatite in Monarch Canyon yielded a K–Ar date of 30 m.y. (Wasserburg *et al.,* 1959), which may correspond to the time of mineralization and retrograde metamorphism. Regional metamorphism may have occurred at the same time (late Mesozoic) as the metamorphism of the nearby Panamint Mountains (see Labotka *et al.*, 1980).

Methods

Analytical data were obtained by wavelength-dispersive electron microprobe analysis on a Materials Analysis Corporation Model #5-SA3 fully automated microprobe. Standard operating conditions are 15kV accelerating potential, 15 nA specimen current (brass), 15–200 sec counting time (counting statistics of 1% S.D.), on-line data reduction using the method of Bence and Albee (1968) and the correction factors of Albee and Ray (1970). Reproducibility in the Caltech lab is within 1 to 2% for major elements and 10% for minor elements (Champion *et al.*, 1975). Probe data are presented here as points on graphs rather than in tables. Complete analyses may be obtained from the author upon request.

Mineral assemblages in pelitic schists

Samples were collected from several localities in the Chloride Cliff Quadrangle in order to document the mineral assemblages (metamorphic grade) and the reactions responsible for the change in mineral assemblages with increasing metamorphic grade. Siliceous dolomite and calciferous schist are not abundant in the Funeral Mountains, and the majority of

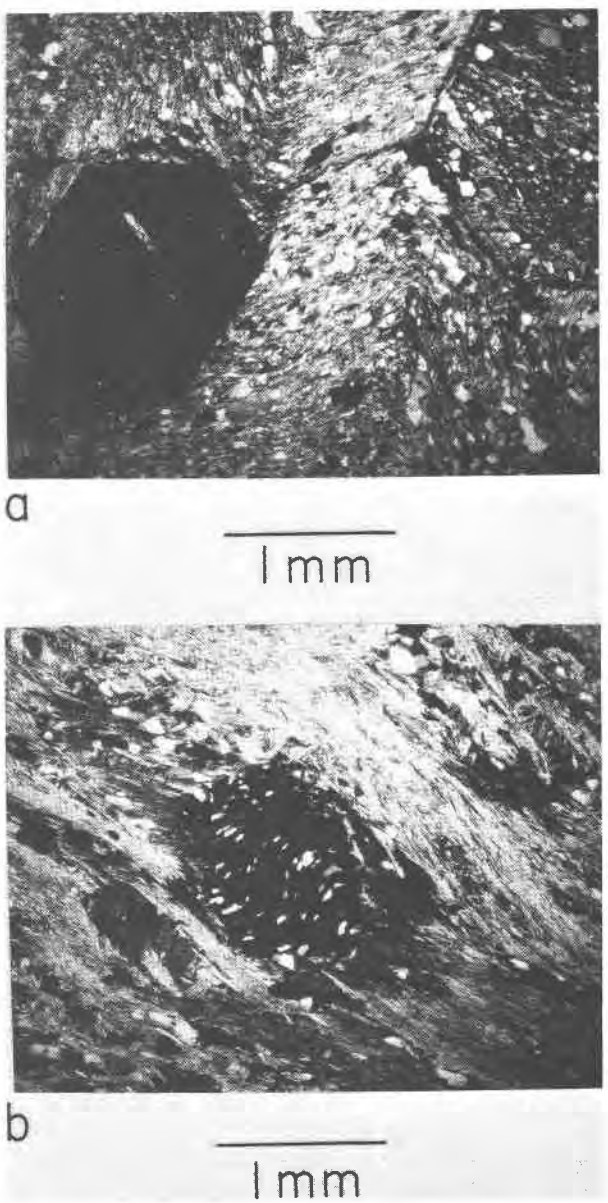

Fig. 3. Textural features of garnet-grade pelitic schists. (a) Relic chloritoid (light) included in garnet (dark) in a garnet + staurolite + chlorite assemblage, FML 85a (crossed nicols). (b) Sigmoidal inclusion trail in garnet (black) in garnet + biotite + chlorite assemblage, CP 45li (crossed nicols).

the rocks collected are pelitic schists from the lower Stirling Quartzite, Johnnie Formation, and the Pahrump Group. On the basis of the mineral assemblages in these pelitic schists, garnet, staurolite + biotite, and kyanite + garnet + biotite isograds were mapped.

The garnet isograd is based on the first appearance of garnet (Fig. 2). The several mineral assemblages observed in the pelitic rocks south of the garnet isograd include:

biotite + chlorite + muscovite + quartz + plagioclase
chloritoid + chlorite + muscovite + quartz + ilmenite

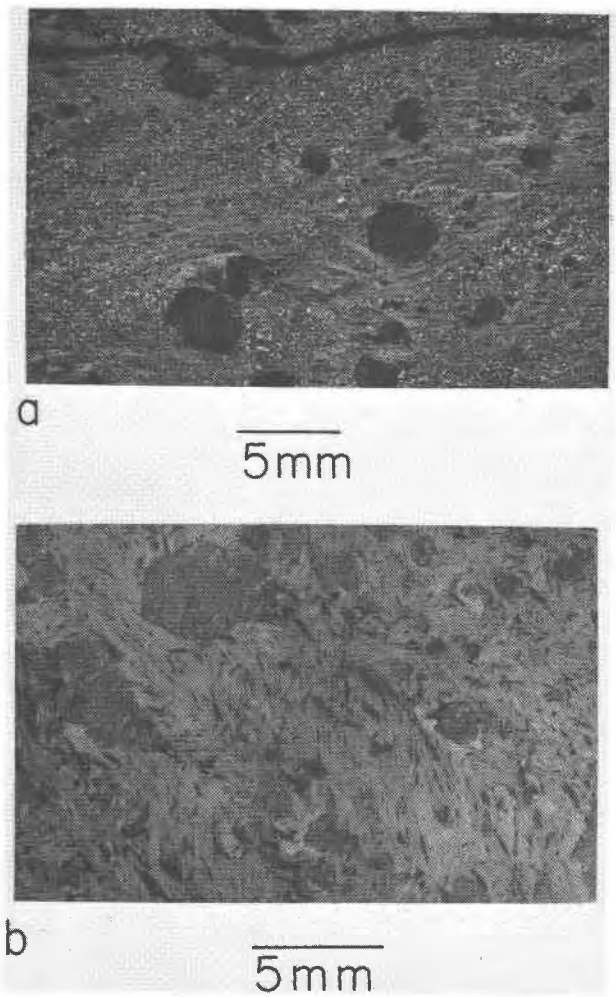

Fig. 4. Development of secondary foliation in pelitic schist. (a) Mica foliation oriented at a high angle to inclusion trails in garnet, CP 45li (crossed nicols). (b) Ilmenite (small black plates) bent into the secondary strain–slip cleavage in a garnet + staurolite + chlorite assemblage, FML 92 (plane polarized light).

chloritoid + chlorite + margarite + muscovite + quartz + rutile
chloritoid + chlorite + kyanite + muscovite + quartz + rutile + hematite

Most of these assemblages represent relatively aluminous rock compositions, and the absence of garnet-bearing assemblages may be due in large part to inappropriate rock compositions. These rocks are relatively fine-grained and the largest porphyroblasts, usually kyanite, are less than a few millimeters long. A foliation defined by a preferred orientation of micas is present, and this foliation is oriented approximately parallel to compositional layering. In many samples the foliation is broadly folded on a small scale, and axial planes of these microfolds lie at a high angle to the foliation. Chloritoid and kyanite porphyroblasts are randomly oriented, although in one sample (FML 66) chloritoid plates appear to have been rotated into the folded foliation.

Rocks in the garnet zone also contain a wide variety of mineral assemblages, but the zone is characterized by the coexistence of garnet and chlorite. Chloritoid occurs in rocks just north of the garnet isograd, and the assemblages found in the lower-grade part of the garnet zone include:

garnet + chlorite + biotite + muscovite + quartz + plagioclase + ilmenite
garnet + chlorite + chloritoid + muscovite + quartz + ilmenite + paragonite
kyanite + chlorite + chloritoid + muscovite + quartz + hematite + rutile
kyanite + chlorite + staurolite + muscovite + quartz + hematite + rutile

The rocks are generally fine-grained and weakly to moderately foliated. Two foliations are apparent. The earlier is defined by a crude parallel alignment of fine-grained micas, oriented approximately parallel to bedding. A second foliation is expressed by gentle crenulation of the first, but in some cases the second foliation is defined by a parallel alignment of medium-grained muscovite, oriented at a high angle to the first. The secondary foliation is not penetrative, but micas occur in 1 to 2 mm wide zone separated by 5 mm intervals. Garnet porphyroblasts, less than 3 mm in diameter, contain quartz inclusion trails which are parallel to the first foliation, but the porphyroblasts had grown prior to the development of the secondary foliation (CP 451i, Fig. 3).

Retrograde textures were identified only in chlori-

toid + kyanite + chlorite assemblages, in which mm-sized magnetite grains are rimmed by hematite, although chloritoid is locally coated by hematite or goethite.

Farther northwest chloritoid-bearing assemblages are absent, and the assemblage garnet + chlorite + staurolite + muscovite + quartz + plagioclase + ilmenite is dominant. Many of the garnet porphyroblasts have inclusions of chloritoid, but chloritoid is absent from the matrix (FML 85a, Fig. 3). The grain size is larger than in the lower-grade part of the garnet zone and staurolite and garnet porphyroblasts several mm in diameter occur. The crenulation cleavage is also better developed and the order of development: primary foliation, porphyroblast growth, crenulation, is observed.

Although staurolite is first encountered in what is here called the garnet zone, the staurolite + biotite isograd is defined on the basis of the first occurrence of the association staurolite + biotite. Figure 2 illustrates the occurrence of garnet + chlorite *vs.* staurolite + biotite assemblages and the staurolite isograd. The assemblages observed in staurolite-grade schists include

I: garnet + staurolite + biotite + muscovite + quartz + plagioclase + ilmenite
II: garnet + staurolite + biotite + chlorite + muscovite + quartz + plagioclase + ilmenite
III: garnet + staurolite + biotite + kyanite + muscovite + quartz + plagioclase + ilmenite

These schists are very coarse-grained and staurolite porphyroblasts several cm long are not uncommon. Staurolite and kyanite tend to be aligned in the foliation. Kinking and crenulation in the schistosity is prominent, and kyanite grains are kinked and ilmenite grains are bent into the crenulation (Fig. 4). Staurolite engulfs and includes garnet, and garnet porphyroblasts that occur in assemblages II and III are greatly embayed, and irregular in form. These textures suggest that garnet is metastable in assemblages II and III and has not been completely digested.

The kyanite + garnet + biotite isograd is defined by the disappearance of staurolite, which is indicated by the stable coexistence of garnet + biotite + kyanite (Fig. 2). The commonly observed pelitic assemblage is garnet + biotite + kyanite + muscovite + quartz + plagioclase + ilmenite + rutile. In Monarch Canyon sillimanite also occurs in this assemblage. Gneissic foliation characterizes the texture of the highest-grade rocks, and migmatites which exhibit passive flow folds and ptygmatic folds occur in Monarch Canyon (Fig. 5).

In thin section garnet porphyroblasts contain large inclusions of biotite and some staurolite, and garnet has preserved the relic composition of biotite and staurolite. Sillimanite generally occurs as needles in quartz, in the vicinity of kyanite grains.

The change in mineral assemblages and the preservation of relic minerals as inclusions in porphyroblasts are indicative of prograde metamorphic reactions. The variety in rock compositions in the Funeral Mountains allows the determination of the distribution of elements in pelitic schists and the elu-

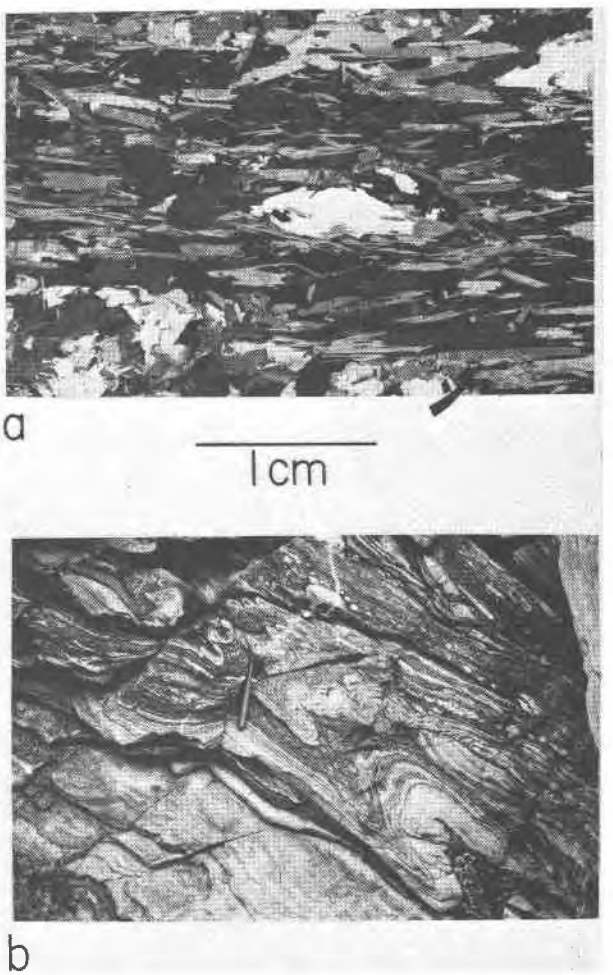

Fig. 5. High-grade rocks in Monarch Canyon. (a) Kyanite + garnet + biotite schist, FML 116b (crossed nicols). Kinkbands may be observed in kyanite grains (lower right, arrow). (b) Migmatite in Monarch Canyon. Melanocratic layers consist of biotite + epidote + plagioclase + quartz, whereas the leucocratic layers are generally devoid of biotite.

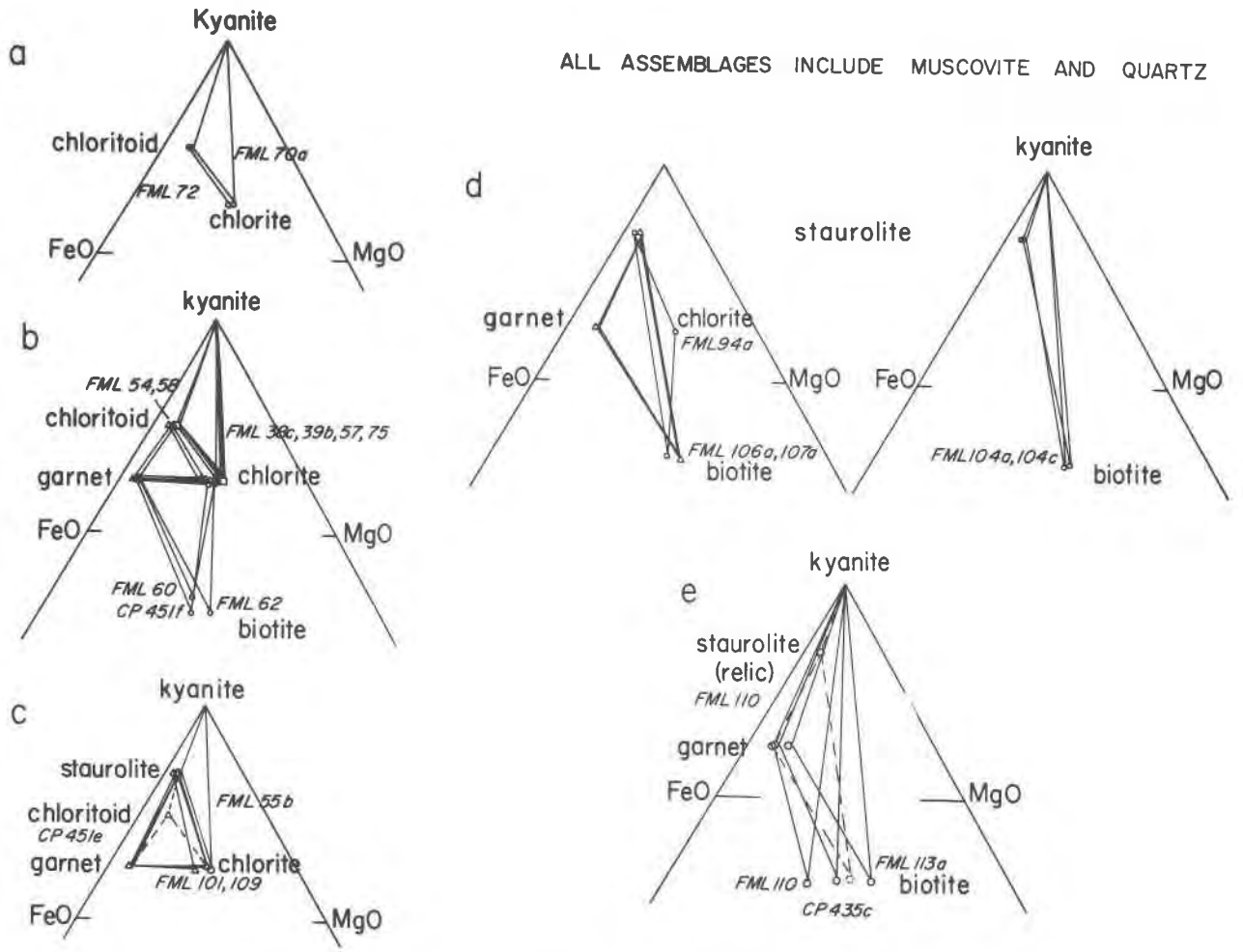

Fig. 6. Compositions of minerals in pelitic schist assemblages plotted in AKFM space, projected from muscovite + quartz. (a) Low-grade assemblages. (b) Assemblages from the lower-grade part of the garnet zone. (c) Assemblages from the higher-grade part of the garnet zone. (d) Staurolite-zone assemblages. (e) Kyanite-zone assemblages. Dashed lines connect compositions of phases that occur as relic inclusions.

cidation of reactions which alter the stable mineral association with increasing grade.

Distribution of elements in pelitic schists

AFM phases

Most of the phases in these rocks can be described in terms of the oxides SiO_2–Al_2O_3–MgO–FeO–H_2O, and the mineral assemblages that occur in quartz + muscovite schists may be represented on the plane Al_2SiO_5–FeO–MgO. The use of this projection as a phase diagram is discussed by Thompson (1957). The range in bulk composition is sufficient to allow the determination of the complete facies types for this system at some grades and of the reactions responsible for the changes in topology with increasing grade.

Analyzed mineral assemblages in pelitic schists from the Funeral Mountains are illustrated in Figure 6 and Table 1. The relative distribution of Fe, Mg, and Al among phases within any one mineral assemblage is consistent in all rocks exhibiting that assemblage. For a given assemblage, tie lines do cross, but these minor inconsistencies are attributed to minor variations in P, T, and a_{H_2O}. For all rocks found within a small area and within the same zone, unlike assemblages do not occupy overlapping regions in composition space, and these changes in mineral assemblage are attributable to changes in bulk composition. Four-phase assemblages occur in some of the

Table 1. Analyzed samples, Funeral Mountains

SAMPLE	QTZ	MUSC	BIO	GA	CH	CTD	ST	KY	SIL	PLAG	ILM	RUT	HEM	MAG	Other	Location	Grade
CP 435c	X	X	X	X				X		X	X					1	K
CP 451e	X	X		X	X	X	X			X	X					12	G
CP 451f	X	X	X	X	X					X	X					12	G
FML 37b	X	X			X	X		X					X	X		9	G
FML 38c	X	X			X	X		X					X			9	G
FML 39b	X	X			X	X		X					X			9	G
FML 54	X	X		X	X	X					X					8	G
FML 55a	X	X						X					X			7	G
FML 55b	X	X			X		X	X				X	X			7	G
FML 56	X	X		X	X					X	X					11	G
FML 57	X	X			X	X		X				X	X	X	par	11	G
FML 58	X	X		X	X	X					X					11	G
FML 60	X	X	X	X	X					X	X					10	G
FML 62	X	X	X	X	X					X	X					10	G
FML 70a	X	X			X	X		X				X	X	X		13	G
FML 72	X	X			X	X						X			marg	13	G
FML 75	X	X			X	X		X					X			6	G
FML 94a	X	X	X	X	X		X			X	X					5	G
FML 101	X	X		X	X		X				X					4	G
FML 104a	X	X	X	X			X	X		X						3	S
FML 104c	X	X	X	X			X	X		X		X				3	S
FML 106a	X	X	X	X			X			X	X					3	S
FML 107a	X	X	X	X			X			X						3	S
FML 109	X	X		X	X		X			X	X					4	G
FML 110	X	X	X	X			X	X	X		X	X				2	K
FML 113a	X	X	X	X				X		X	X					1	K
FML 116b	X	X	X	X				X		X	X					1	K

All minerals except quartz were analyzed.
Par = paragonite, marg = margarite; K-kyanite, s-staurolite, G-garnet; locations shown on Fig. 2.

higher-grade rocks, but the garnet in the staurolite-zone assemblage garnet + staurolite + biotite + chlorite appears to be altered and the garnet is believed to be relic. Likewise staurolite in kyanite + garnet + biotite zone assemblages occurs only as inclusions in garnet or large muscovite plates, and the staurolite also appears to be a relic phase. This apparent consistency in the relative order of element partition and with the Gibbs phase rule suggests that chemical equilibrium was closely approached during metamorphism and invites a closer examination of the mineral chemistry and its relation to rock composition and metamorphic grade.

Chlorite is the most common mineral in the lower metamorphic grades, and its major-element chemistry is illustrated in Figure 7. The range in total Al is relatively small and varies from 2.7 to 3.0 cations/formula. Chlorite that coexists with biotite tends to be less aluminous than chlorite that coexists with more aluminous minerals. Chlorite with the ideal composition of $(Mg,Fe)_{6-x}Al_x^{VI}(Si_{4-x}Al_x^{IV})O_{10}(OH)_8$ should fall on the line $Al^{IV} = Al^{VI}$. Most analyzed chlorite corresponds to this expectation, but the substitution of up to $0.2Fe^{3+}$ cations/formula for Al^{VI} is indicated for analyses which contain an excess of Al^{IV} over Al^{VI}, and those analyses which shown an excess of Al^{VI} suggest the substitution $2Al^{VI} + \square^{VI} \rightleftarrows 3Fm^{VI}$.

Garnet shows a larger range in composition than chlorite, but this range is principally due to the additional components MnO and CaO. All analyzed garnets are essentially stoichiometric $(Fe,Mg,Mn,Ca)_3Al_2Si_3O_{12}$; the amounts of TiO_2 and Cr_2O_3 are generally less than can be detected by the probe. Garnet grains are chemically zoned (Fig. 8) and the greatest deviations from almandine–pyrope solid solutions are observed in garnet-grade samples. The maximum amount of measured grossular is 20 mole % and up to 19 mole % spessartine is observed. Garnet zoning patterns are of two types. In both types manganese decreases from core to rim, but calcium is observed to decrease or increase from core to rim.

Nearly all zoning patterns encompass compositional changes of less than 5 mole % for grossular or spessartine components. The change in grossular and spessartine is generally balanced by a complementary change in the almandine component, and pyrope remains relatively constant. The decrease in

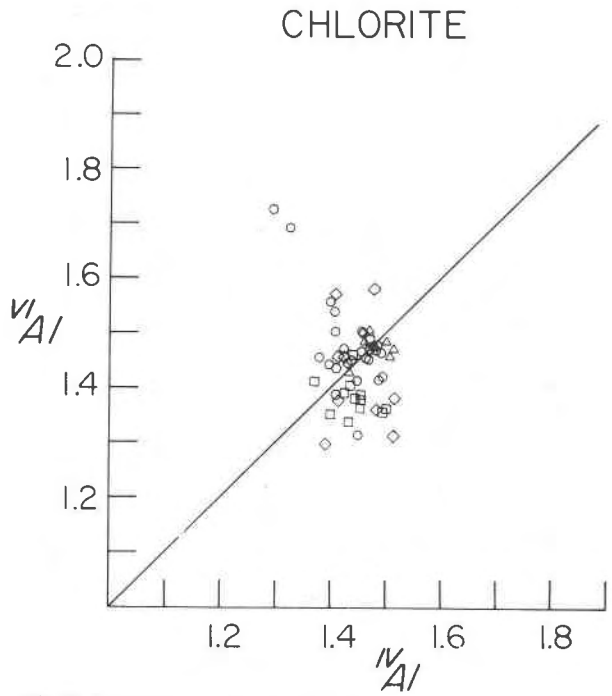

Fig. 7. Al content of chlorite. The line represents compositions generated by the substitution $^{IV}Al + {}^{VI}Al \leftrightarrows {}^{IV}Si + {}^{VI}Mg$. Symbols indicate nature of coexisting phases. Circle : + kyanite triangle: + garnet + chloritoid; square: + garnet + biotite; diamond: + garnet + staurolite; hexagon: + staurolite + biotite. Units are cations/formula unit.

Mn from core to rim is most likely attributable to a Rayleigh-fractionation process during garnet growth (Hollister, 1966), because garnet is essentially the only Mn-phase present. Ilmenite may contain up to 2 wt. % MnO, but all other phases show only barely detectable amounts of manganese; the variations in Ca content may be related to continuous and discontinuous reactions involving plagioclase, and will be examined in greater detail below.

Pyrope increases from about 5 mole % to 20 mole % with increasing grade, and the compositional range encompassed by garnet zoning decreases with increasing grade.

The distribution of Fe, Mg, Mn, and Ca between garnet rims and coexisting chlorite is shown in Figure 9. Chlorite consists essentially of Fe and Mg but garnet contains substantial amounts of Ca and Mn as well. In the Ca-free system, the most Fe-rich chlorite coexists with garnet that contains no Mn. As the amount of Mn in garnet increases, so does the amount of Mg in chlorite. Similar relations hold in the Mn-free system. The occurrence of apparently crossing tie lines can arise by the addition of Ca to garnet as well as to the change in the intensive parameters P, T, and a_{H_2O}.

The variations in biotite chemistry are illustrated in Figure 10. The range in biotite compositions is quite limited. Mg/(Mg + Fe) varies between 0.40 and 0.60 and the Mg/Fe of biotite depends greatly on metamorphic grade and mineral assemblage (consult Fig. 6). The partition of Fe and Mg between garnet and biotite has a strong dependence upon temperature, and will be examined more closely in order to estimate the temperature of metamorphism. The Al content of biotite is confined to the range 1.6 to 1.7 cations/formula, but nearly all analyses show an excess of Al^{VI} over Al^{IV}. There is an observed excess of up to 0.35 Al^{VI}/formula over the amount required by the substitution $Al^{VI} + Al^{IV} \rightleftarrows Fm^{VI} + Si^{IV}$ and a substitution of up to approximately 0.17 mole % dioctahedral mica is suggested.

Biotite from garnet- and staurolite-grade samples contains a uniform level of Ti, ranging from 0.08 to 0.11 cations/formula (~1.5 to 2.0 wt. % TiO_2). In these assemblages ilmenite is the saturating Ti phase, but kyanite-zone biotite from rutile-bearing assemblages contains up to 0.19 cations Ti/formula (~3.25 wt. % TiO_2).

The Na content in biotite is low and Na/(Na + K) ranges from 0.02 to 0.06 ($Na_2O < 0.4$ wt. %). Biotite from staurolite-zone assemblages tends to have more Na_2O than biotite from garnet- or kyanite-zone assemblages. Ca is below the detection limit of the microprobe.

Chloritoid and staurolite consist essentially of FeO, MgO, Al_2O_3, SiO_2, and H_2O. Mn usually occurs in amounts less than 0.2 wt. % in staurolite and less than 0.4 wt. % in chloritoid. Zn also occurs in these small amounts except in staurolite from FML 55b, which has 2.5 wt. % ZnO. Up to 0.5 wt. % TiO_2 is present in staurolite. The amounts of Mn and Zn are very small (except in garnet cores) so that the ratios Mn/Fe and Zn/Fe encompass the range 0.0 to 0.01. Nothing can be said confidently regarding the relative partitioning of these elements except that garnet concentrates Mn and staurolite concentrates Zn.

The principal variations in the chemistry of these minerals is in the Mg/Fe ratio. Figure 11 illustrates the regular distribution of Fe and Mg among coexisting mafic phases. Chlorite is always the most Mg-rich and biotite is always slightly more Fe-rich. Garnet is the most Fe-rich phase and chloritoid and staurolite have Mg/Fe values intermediate to garnet and biotite. The relative partition of Fe and Mg between

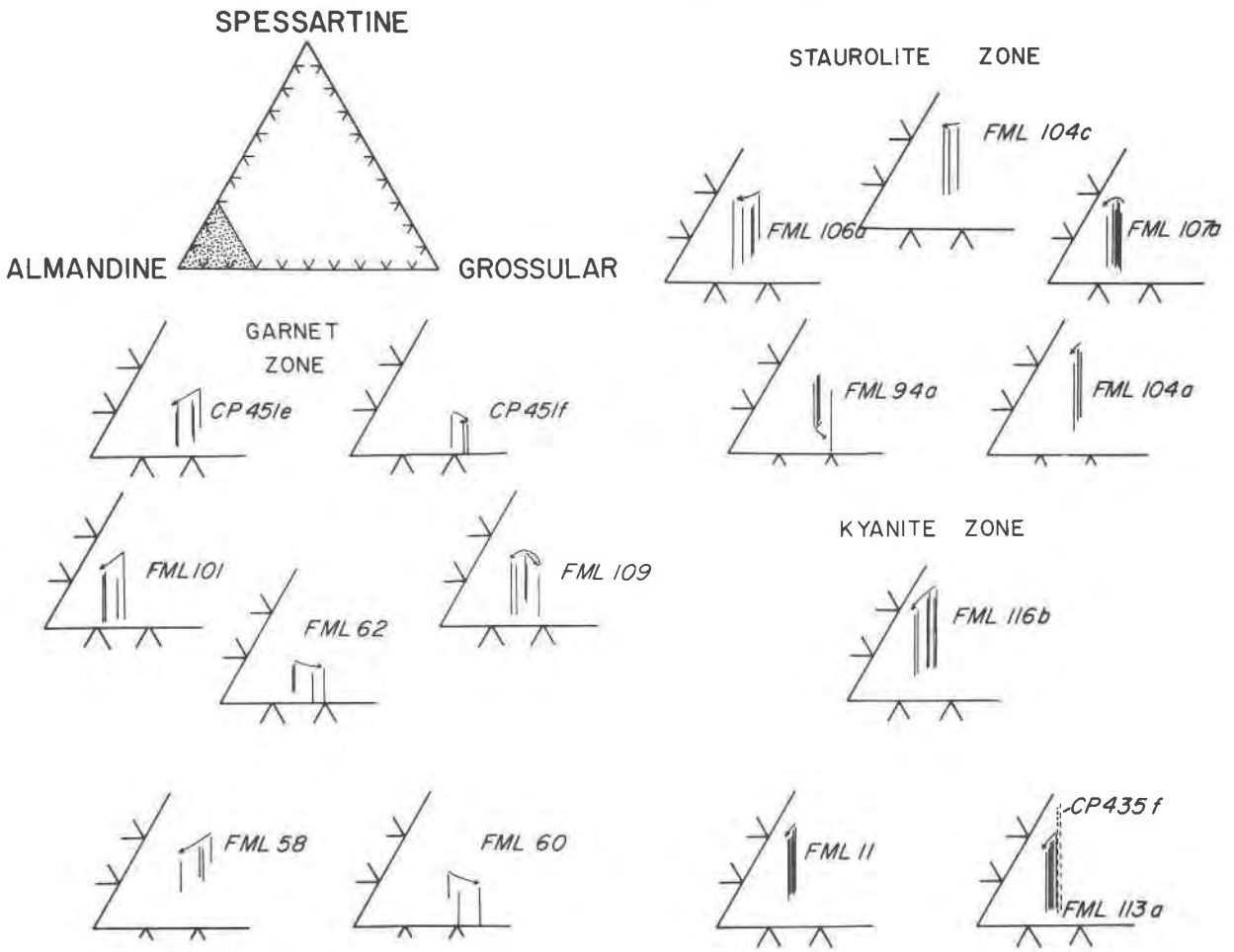

Fig. 8. Garnet compositions all fall in the region mole % almandine > 70%. Length of line represents the amount of pyrope. Arrows indicate direction of zoning from core to rim.

chloritoid and staurolite is difficult to assess because coexisting chloritoid and staurolite have not been observed. In one sample (CP 451e) chloritoid occurs as inclusions in garnet in a garnet + staurolite + chlorite assemblage, and staurolite is more Fe-rich than chloritoid, which is consistent with the observations in Panamint Mountains assemblages (Labotka, 1980) and the suggestions of Albee (1972). Not only is the order of Fe enrichment chlorite < biotite < chloritoid < staurolite < garnet observed, but the distribution coefficients [$K_D \equiv (Mg/Fe)^{\alpha}/(Mg/Fe)^{\beta}$] show only small variations [equal distances between two minerals represent equal K_D because $\log K_D = \log (Mg,Fe)^{\alpha} - \log (Mg/Fe)^{\beta}$]. This relative consistency in Fe and Mg partition among coexisting mafic phases and constancy of total Al content in biotite and the relatively regular Al content in chlorite suggest chemical equilibrium was closely approached during metamorphism. The small variations in K_D (Fe/Mg) are attributable to variations in the intensive thermodynamic parameters, or especially in the case of garnet to the addition of Ca and Mn.

Note that in sample FML 94a, in which on a textural basis garnet is interpreted to be a relic in the assemblage staurolite + chlorite + biotite, the garnet rim is more Mg-rich than staurolite. This observation is contrary to the common observation that garnet is the more Fe-rich mineral, and this apparent reversal in K_D is consistent with the interpretation that garnet is not stable in this assemblage.

Na K Ca phases

Most assemblages contain three AFM phases in addition to muscovite and quartz and are invariant to small arbitrary changes in intensive variables. Most rocks contain Na and Ca as additional components,

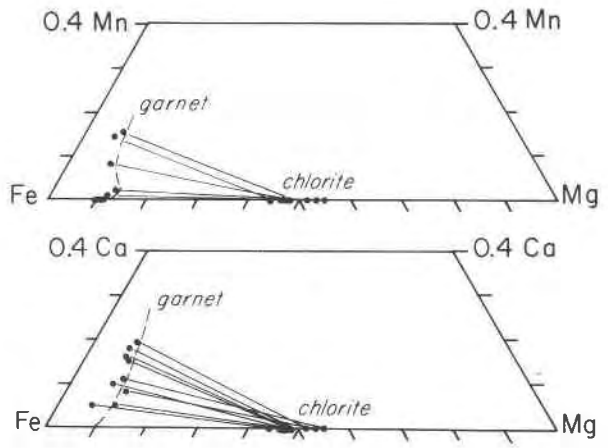

Fig. 9. Distribution of Mn, Ca, Fe, and Mg between coexisting garnet and chlorite.

and here the nature of the saturating phases is considered. In the Funeral Mountains plagioclase, paragonite, and margarite occur as the Na- and Ca-saturating phases.

Muscovite occurs in all assemblages in a variety of textures ranging from fine-grained sericite to coarse plates. The composition deviates only slightly from $KAl_3Si_3O_{10}(OH)_2$, as shown in Figure 12. Na substitutes for K in amounts up to 0.15Na/(Na + K) in lower-garnet-grade samples and approximately 0.25 in muscovite coexisting with paragonite (?). The Na content is up to 0.3Na/(Na + K) in the higher-grade samples.

The amount of phengite substitution is likewise small. The maximum amount of Si observed is 3.12/formula in garnet-grade samples and about 3.06/formula in staurolite- and kyanite-grade samples. In the low-grade assemblages, muscovite coexisting with biotite contains more of the $Si^{IV} + Mg^{VI} \rightleftarrows Al^{IV} + Al^{VI}$ substitution than muscovite from biotite-absent assemblages. All higher-grade assemblages contain biotite, which suggests that with increasing grade the phengite content of muscovite decreases.

The excess SiO_2 in muscovite is balanced by the substitution of FeO and MgO for octahedral Al. Muscovite analyses indicate 0.5 to 0.6 wt. % MgO and 1.0 to 2.5 wt. % "FeO". Most of the iron appears to be ferric because the excess silica is nearly balanced by the MgO present and the total positive change indicated is nearly always less than the theoretical value of 22.0. Muscovite from hematite-bearing assemblages tends to contain more "FeO" (nearly all of which must be Fe_2O_3) than muscovite from hematite-free assemblages.

Paragonite has been tentatively identified in FML 58, which contains the assemblage garnet + chloritoid + chlorite. The sample has not been X-rayed, but during microprobe analysis of fine-grained white mica, a Na-rich K-poor mica was encountered. The cation sum of Na + K + Ca is much less than one, and the ratio Na/(Na + K + Ca) was estimated with the assumption that only Na was lost during analysis. A systematic search for paragonite has not been performed, so its distribution among different assemblages is unknown.

Margarite occurs in one low-grade assemblage with chloritoid + chlorite (FML 72). The margarite appears as ~ 2 mm blades in a fine-grained matrix.

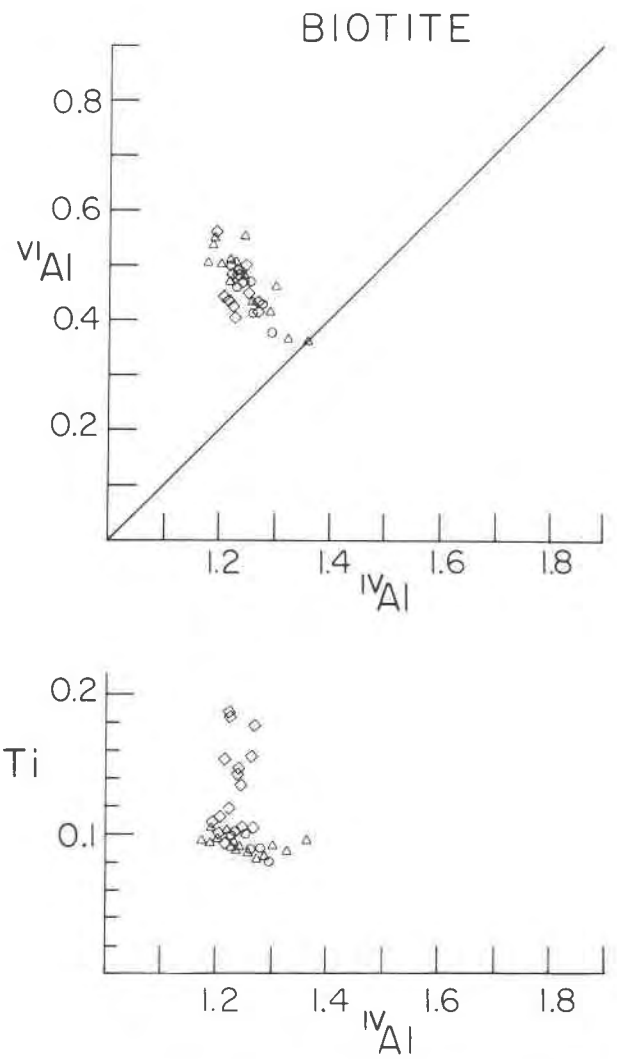

Fig. 10. Al and Ti content of biotite. Nearly all analyses indicate an excess of octahedral Al which suggests the importance of the substitution $^{VI}\square + 2^{VI}Al \leftrightarrows 3^{VI}Mg$. Symbols indicate grade of samples. Circle: garnet zone; triangle: staurolite zone; diamond: kyanite zone. Units are cations/formula unit.

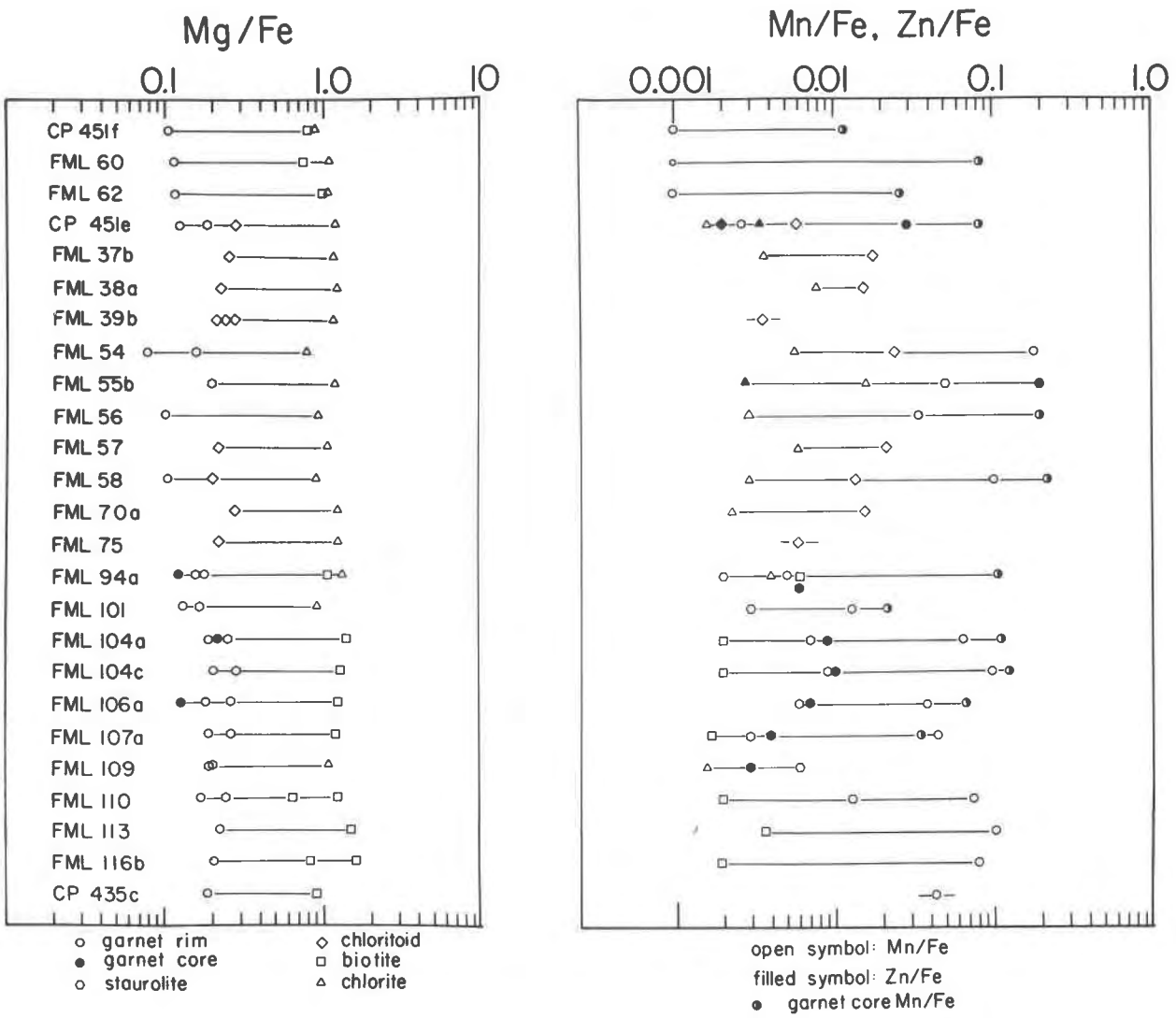

Fig. 11. Distribution of Fe, Mg, Mn, and Zn between coexisting minerals. The data indicate that the order of Fe enrichment is chlorite < biotite < chloritoid ≤ staurolite < garnet. Garnet concentrates Mn, staurolite concentrates Zn.

The distribution of Na, Ca, and K in coexisting white micas is illustrated in Figure 13, which shows that even muscovite coexisting with margarite contains no calcium.

Plagioclase occurs in most assemblages except chloritoid + chlorite + kyanite and garnet + chlorite + chloritoid. Plagioclase in garnet-grade samples tends to form rounded porphyroblasts which contain quartz inclusions. Plagioclase in staurolite- and kyanite-grade samples occurs in twinned grains in a quartz–plagioclase mosaic.

The compositions of plagioclase and coexisting muscovite are shown in Figure 14. Plagioclase contains essentially no K and the observed compositional range is An_{60} to An_8. Zoning and grain-to-grain compositional variations are small except as noted below. In FML 56 plagioclase An_{35} occurs with plagioclase An_8. The plagioclase contains multitudinous inclusions and only one plagioclase of composition An_8 was observed. Hence it is difficult to determine whether the two compositions coexist due to immiscibility or whether the two are related by zoning or reaction. No other samples were observed with this relation.

The plagioclase in sample FML 60 is the most calcic feldspar observed and exhibits zoning from a Ca-rich core (An_{60}) to a more sodic rim (An_{45}). This sample contains the most Ca-rich garnet which is

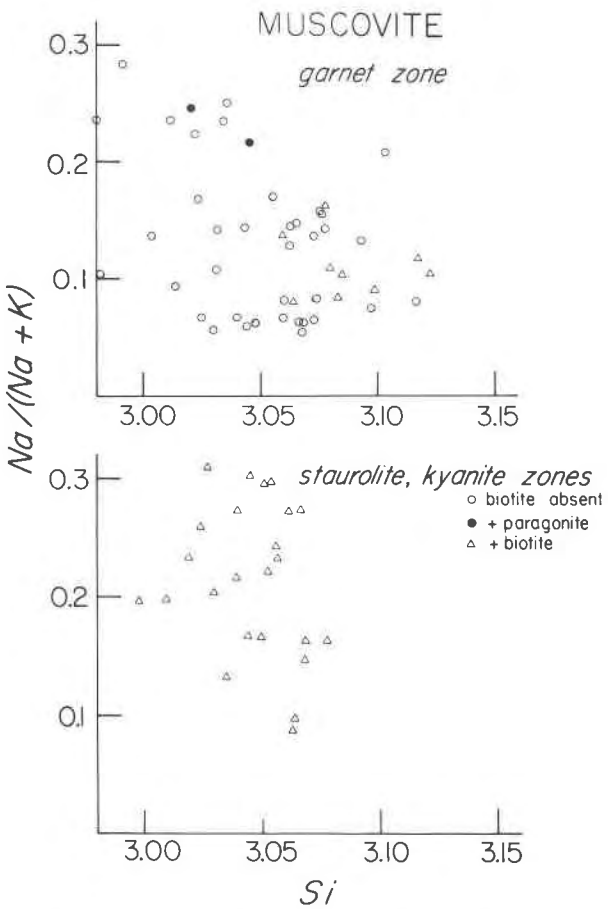

Fig. 12. Paragonite (Na) and phengite (Si) contents of muscovite.

zoned (Fig. 8) toward more Ca-rich compositions, opposite to the plagioclase zoning pattern. Figure 15 shows that the more Ca-rich garnets tend to coexist with more Ca-rich plagioclase, and that because these are the only Ca phases present their Ca content is controlled to some degree by the amount of Ca in the total rock. Among these garnet-grade samples there is a fairly regular relation between the Na/(Na + Ca + K) ratios in muscovite and coexisting feldspar. The more Na-rich muscovites tend to coexist with the more Na-rich feldspars. Staurolite- and kyanite-grade samples contain plagioclase in the compositional range An_{15} to An_{25} and coexisting muscovite is correspondingly more Na-rich (Fig. 14).

Fe-Ti phases

All mineral assemblages contain Fe–Ti phases. Ilmenite is the most common, and it occurs in the assemblages garnet + chlorite + biotite, garnet + chlorite + chloritoid, and garnet + staurolite + chlorite in the garnet zone, and in the higher-grade assemblages garnet + staurolite + biotite, staurolite + biotite + chlorite, kyanite + staurolite + biotite, and kyanite + garnet + biotite. Every ilmenite analysis shows more Ti than required by $FeTiO_3$, and the presence of minute rutile lamellae is indicated. In general MgO occurs in amounts less than 0.1 wt. % and MnO less than 1.0 wt. %. The maximum MnO observed is 2.0 wt. %.

Rutile occurs in the low-grade assemblage kyanite + chlorite + chloritoid, and the high-grade assemblages kyanite + staurolite + biotite and kyanite + garnet + biotite.

Ferric-iron phases are observed in only the assemblage kyanite + chlorite + chloritoid. Hematite occurs as small (<0.5 mm) plates and as pseudomorphs after magnetic cubes. The remnant magnetite is essentially pure Fe_3O_4 and the hematite rim on magnetite is pure Fe_2O_3. The smaller matrix hematite plates apparently contain up to 50 mole % $FeTiO_3$ (Fig. 16). Most of these associations contain rutile in addition. The unusually high TiO_2 content in hematite suggests that there are minute ilmenite lamellae present which may have exsolved during retrograde metamorphism.

Mineral facies and reactions

The range in bulk composition and metamorphic grade provide a surprisingly complete determination of mineral facies in a Barrovian metamorphic terrane. The details of the facies types which involve Ca, Na, Fe^{3+} phases are at present only sketchy, but enough information exists to suggest the phase relationships. Figure 17 illustrates the generalized facies

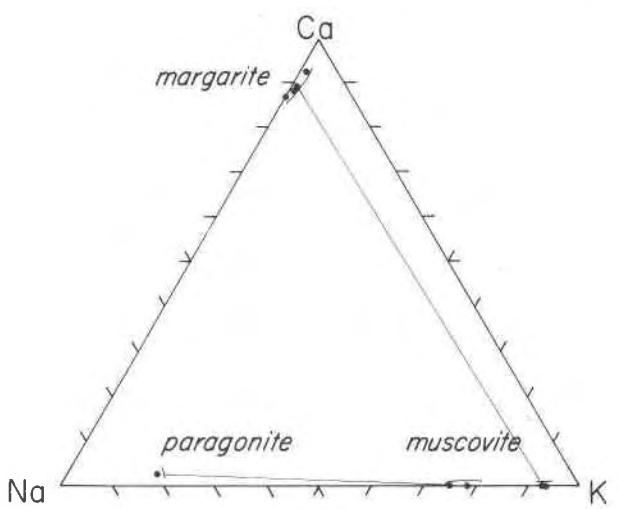

Fig. 13. Distribution of Na, Ca, and K between coexisting white micas.

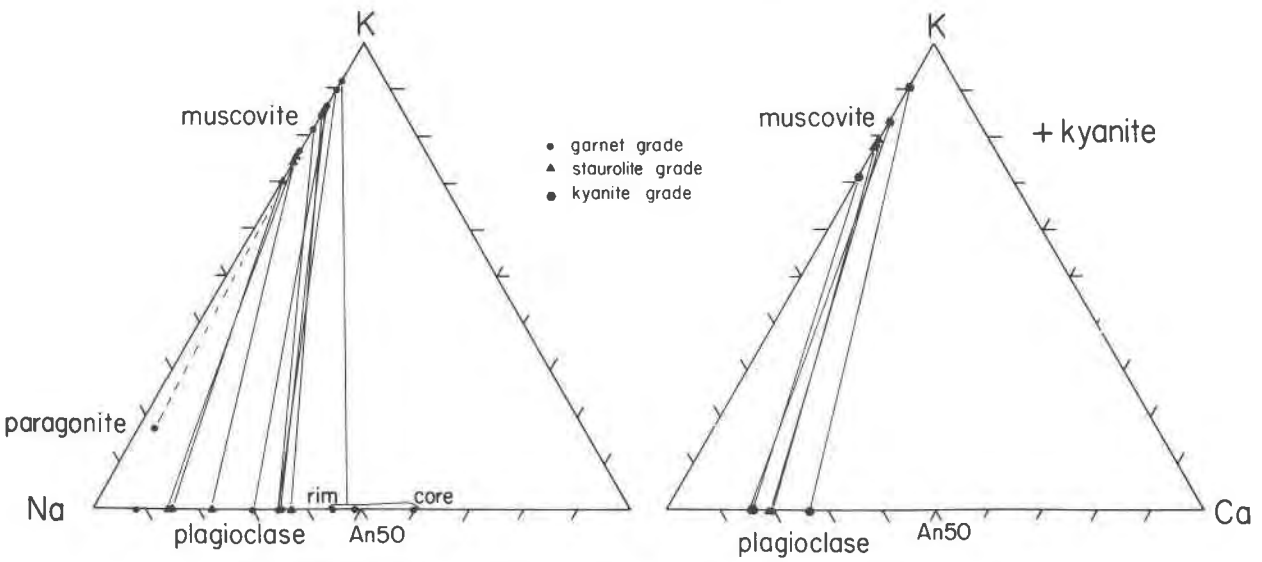

Fig. 14. Distribution of Na, Ca, and K between coexisting muscovite and plagioclase.

types which describe the distribution of elements among coexisting facies during the metamorphism of the Funeral Mountains.

These AKFM mineral facies are very similar to those exhibited by other Barrovian terranes where the complete facies types have been determined, principally in the New England regional-metamorphic terrane. The assemblages in garnet-grade rocks from Indian Pass are identical to those found at Mt. Grant in Vermont [Albee (1965), and Fig. 17]. Even the incomplete information regarding the saturating Fe^{3+}, Ti, and Na phases is compatible with the Mt. Grant assemblages. By analogy, the undetermined phases may be assigned. Magnetite should occur in the assemblages garnet + chlorite + chloritoid and garnet + chlorite + biotite; paragonite should occur in the assemblage kyanite + chlorite + chloritoid.

The staurolite-zone assemblages shown in Figure 17 are very similar to the assemblages exhibited by the Gassetts Schist, Vermont (Thompson *et al.*, 1977). Ferric-iron phases do not occur in the analyzed samples from the Funeral Mountains, and plagioclase rather than paragonite coexists with kyanite.

Titanium phases occur in all observed assem-

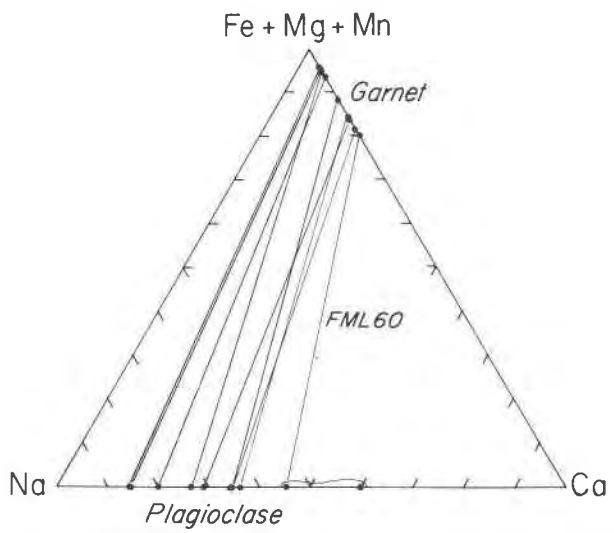

Fig. 15. Partition of Ca between coexisting garnet and plagioclase; the more calcic garnets coexist with more calcic plagioclases.

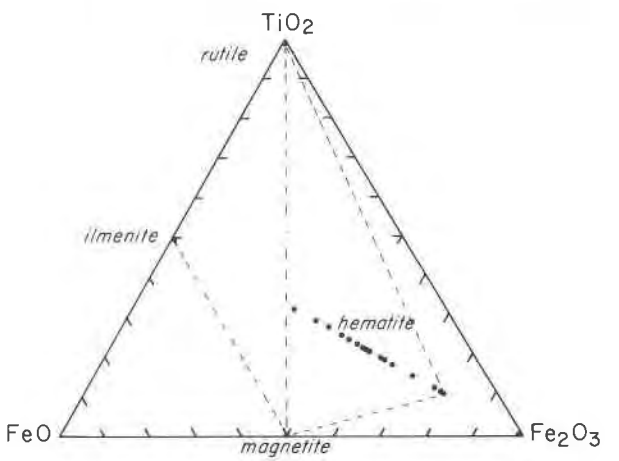

Fig. 16. Composition of Fe–Ti oxides. Hematite shows a wide range in composition due to the analysis of minute ilmenite lamellae. Dashed lines indicate probable phase relations in the low-grade assemblage kyanite + chloritoid + chlorite.

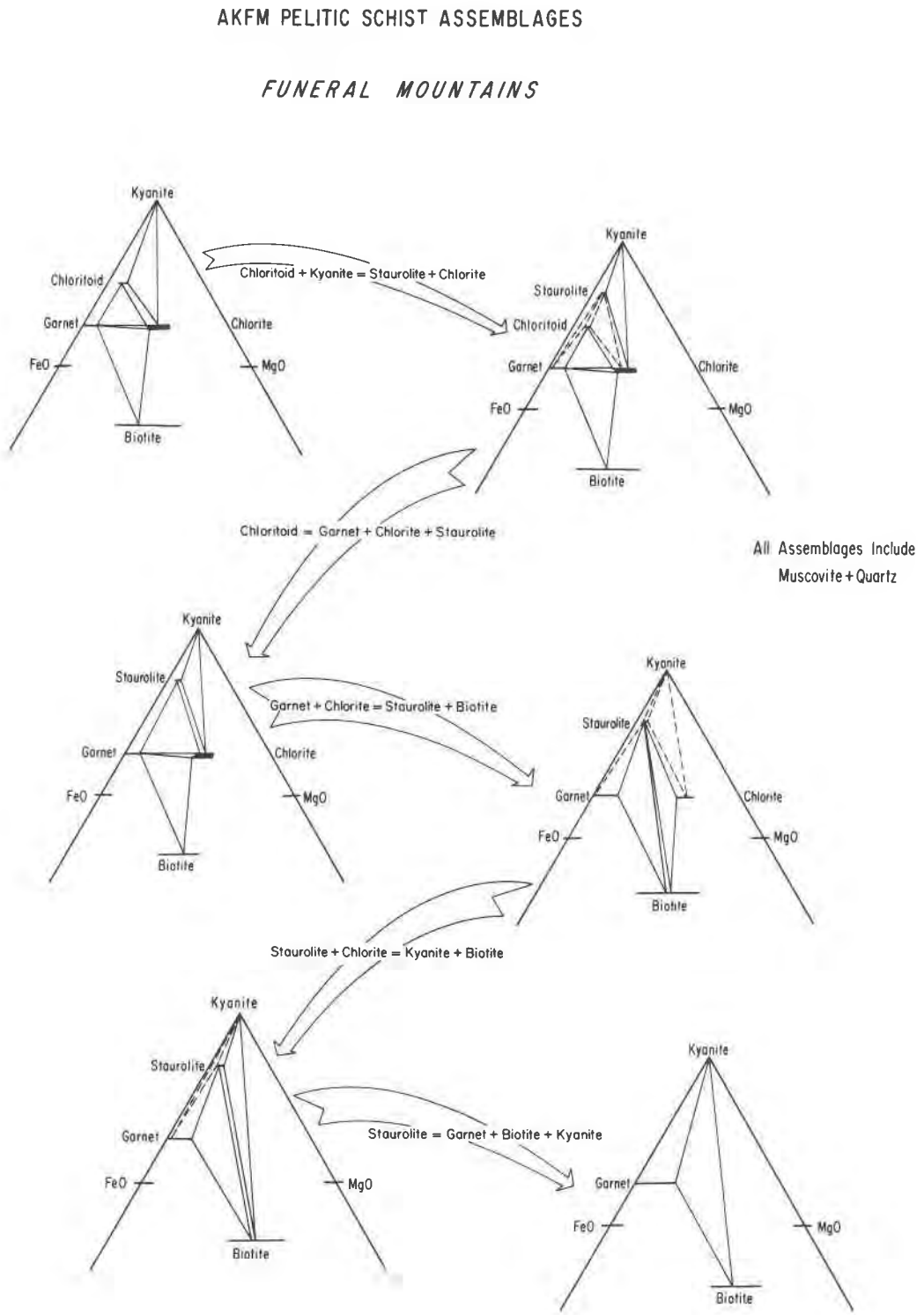

Fig. 17. Generalized AKFM facies series for the metamorphism of pelitic schists in a Barrovian-type terrane. Assemblages indicated by the dashed lines are not observed, but are inferred to have been stable. The inversion from kyanite to sillimanite occurs after the breakdown of staurolite.

blages. Rutile occurs in aluminosilicate-bearing assemblages, whereas ilmenite occurs in all others. The distribution of Fe^{3+} and Na phases among the assemblages is not well documented, but paragonite and magnetite probably may occur in high-Al and low-Al assemblages respectively.

All the assemblages and the sequence of facies types are very similar to those found in the regional metamorphic terranes in northern Vermont (Albee, 1968) and in the Barrovian terrain in Scotland (Harte, 1975), except that staurolite breaks down prior to the kyanite-to-sillimanite transition. Each facies type is related to another by a discontinuous reaction which either represents a change in mineral compatibilities or a termination of a phase. The reactions which relate the changes in facies in the system AKFM are

(1) unknown and probably complex garnet-forming reactions
(2) incoming of staurolite by chloritoid + kyanite = staurolite + chlorite
(3) breakdown of chloritoid by chloritoid = garnet + chlorite + staurolite
(4) break in garnet-chlorite association by garnet + chlorite = staurolite + biotite
(5) elimination of chlorite from most rocks by staurolite + chlorite = kyanite + biotite
(6) breakdown of staurolite by staurolite = garnet + kyanite + biotite
(7) polymorphic inversion of kyanite to sillimanite.

The stoichiometry of each discontinuous reaction may be ascertained by the natural composition data for mineral associations that are stable on either side of an isograd. The present sample density does not permit the determination of the stoichiometry of most reactions, but inclusions of relic mineral phases in garnet suggest the terminal compositions of chloritoid and staurolite.

Sample CP 451e preserves the probable terminal chloritoid as inclusions in garnet in a garnet + chlorite + staurolite assemblage. The compositions of the phases in this sample provide the terminal chloritoid reaction

$$10.0\underset{\text{chloritoid}}{Fe_{1.57}Mg_{0.43}Al_4Si_3O_8(OH)_4} + 4.92\underset{\text{quartz}}{SiO_2}$$
$$+ 1.14\underset{\text{anorthite}}{CaAl_2Si_2O_8} = 3.26\underset{\text{garnet}}{Fe_{2.35}Ca_{0.35}Mg_{0.30}Al_2Si_3O_{12}}$$
$$+ 3.85\underset{\text{staurolite}}{Fe_{1.66}Mg_{0.34}Al_{8.67}Si_4O_{22}(OH)_2}$$
$$+ 0.82\underset{\text{chlorite}}{Fe_{2.04}Mg_{2.47}Al_{1.49}(Al_{1.49}Si_{2.51})O_{10}(OH)_8}$$
$$+ 12.89H_2O$$

Anorthite is derived from plagioclase and such a reaction may cause plagioclase to become more sodic (see discussion below).

The terminal composition of staurolite may also be approximated by the composition of staurolite inclusions in garnet in the garnet + kyanite + biotite assemblage from sample FML 110. The composition of biotite inclusions in garnet is also used because the biotite in the matrix has a significantly different Mg/Fe.

$$10.0\underset{\text{staurolite}}{Fe_{1.65}Mg_{0.35}Al_{8.67}Si_4O_{22}(OH)_2}$$
$$+ 0.91\underset{\text{muscovite}}{KAl_3Si_3O_{10}(OH)_2}$$
$$+ 15.55\underset{\text{quartz}}{SiO_2} = 5.94\underset{\text{garnet}}{Fe_{2.80}Mg_{0.40}Al_2Si_3O_{12}}$$
$$+ 0.91\underset{\text{biotite}}{KFe_{1.16}Mg_{1.24}(Al_{1.74}Si_{2.74})O_{10}(OH)_2} +$$
$$37.96\underset{\text{kyanite}}{Al_2SiO_5} + 10H_2O$$

The reaction has been simplified by combining Ca and Mn in garnet with Fe. Because muscovite is more Na-rich than biotite, and because garnet contains significant Ca, any muscovite-consuming, garnet-producing reaction will be accompanied by an increase in the albite component in plagioclase. If both garnet and muscovite are consumed or produced (as in the crossover garnet + muscovite + chlorite = staurolite + biotite) the composition of plagioclase will not necessarily change.

The compositions of all phases in invariant associations is greatly affected by continuous and exchange reactions. The compositions of most mafic phases become more Mg-rich with increasing grade. Biotite is an exception, and once staurolite breaks down biotite associated with garnet and kyanite becomes more Fe-rich.

The compositions of coexisting muscovite and plagioclase are governed by both exchange and continuous reactions. At low grades, the distribution of sodium between muscovite and plagioclase is represented by

$$NaAl_3Si_3O_{10}(OH)_2 + KAlSi_3O_8 = KAl_3Si_3O_{10}(OH)_2 + NaAlSi_3O_8$$

and

$$NaAl_3Si_3O_{10}(OH)_2 + CaAl_2Si_2O_8 = CaAl_4Si_2O_{10}(OH)_2 + NaAlSi_3O_8$$

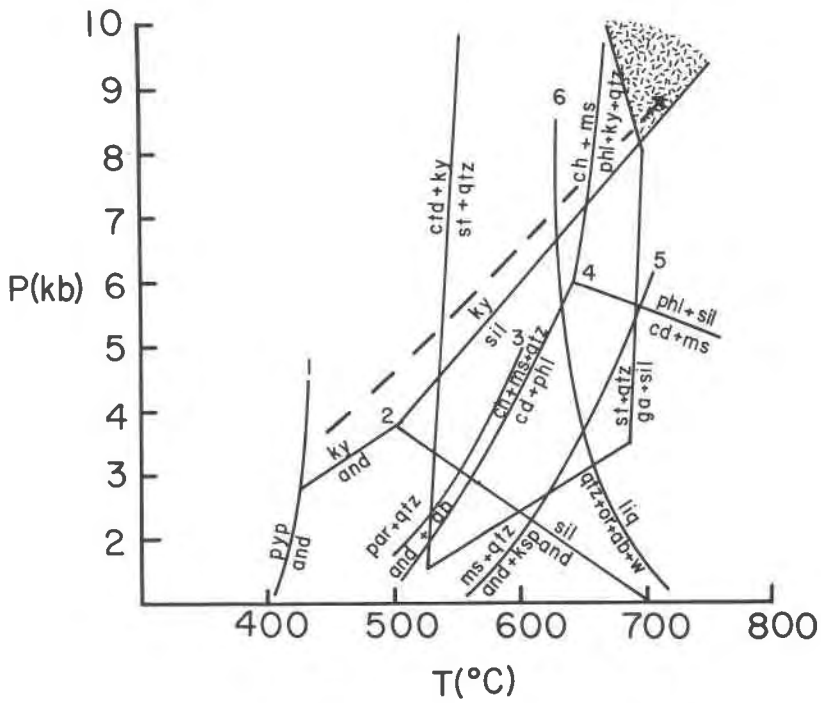

Fig. 18. Extreme conditions of metamorphism based on the correspondence of observed mineral assemblages to experimentally determined phase equilibria. Boundaries taken from (1) Kerrick (1968), (2) Holdaway (1971), (3) Chatterjee (1972), (4) Bird and Fawcett (1973), (5) Chatterjee and Johannes (1974), and (6) Tuttle and Bowen (1958). Staurolite stability from Ganguly (1972).

Because plagioclase contains essentially no K and muscovite contains no Ca, the equilibrium constant for the first reaction is very large and for the second very small. At higher grades plagioclase coexists with kyanite, and the compositions of plagioclase and muscovite coexisting with kyanite and quartz are controlled by the continuous reaction

$$NaAl_3Si_3O_{10}(OH)_2 + SiO_2 = NaAlSi_3O_8 + Al_2SiO_5 + H_2O$$

In the kyanite zone the additional reaction

$$3CaAl_2Si_2O_8 = Ca_3Al_2Si_3O_{12} + 2Al_2SiO_5 + SiO_2$$

affects the calcium distribution between coexisting plagioclase and garnet.

Physical conditions during metamorphism

The values of the intensive thermodynamic parameters may be estimated by comparison of natural mineral associations to experimental data, by calculation using mineral compositions and calibrated geothermometer–barometers, and by inference from the geologic setting.

The critical observations that define the P–T trajectory during metamorphism are that kyanite is the stable aluminosilicate throughout most of the terrane and that staurolite breaks down before kyanite inverts to sillimanite.

The experimental work of Holdaway (1971), Hoschek (1969), Ganguly (1972), and Richardson (1968) (Fig. 18) suggests that within the kyanite stability field minimum conditions at the staurolite isograd are ~550°C, 5 kbar; at the kyanite + biotite isograd ~625°C, 6 kbar; and at the kyanite isograd ~700°C, 8 kbar. These are P–T conditions where $P_{H_2O} = P_T$ and P_{O_2} is at values within the stability field of magnetite. Higher P_{O_2} conditions restrict apparent staurolite stability (Ganguly, 1972), but none of the high-grade rocks contain ferric-iron phases, so that the values estimated by these experiments are appropriate.

Quantitative estimates of the physical conditions can be calculated from existing geothermometers. Temperatures are estimated by the relative partitioning of Fe and Mg between garnet and biotite, from the oxygen isotopic calibration of Goldman and Albee (1977). The distribution coefficient provides temperature estimates for all garnet–biotite assemblages,

Table 2. Garnet–biotite temperatures, Funeral Mountains

SAMPLE	GARNET			BIOTITE				TEMPERATURE*		
	Mg/Fe	X_{Mn}	X_{Ca}	Mg/Fe	X_{Fe}	X_{Ti}	X_{Al}^{VI}	G-A	F-S °C	T
CP 435c	0.192	0.035	0.050	0.973	0.507	0.056	0.154	538	604	645
CP 451f	0.107	0.0	0.182	0.820	0.550	0.033	0.161	488	483	564
FML 60	0.116	0.0	0.198	0.878	0.533	0.028	0.109	487	486	567
FML 62	0.106	0.0	0.159	1.010	0.495	0.030	0.140	443	432	528
FML 104a	0.198	0.051	0.064	1.416	0.414	0.028	0.138	497	501	578
FML 104c	0.205	0.073	0.051	1.302	0.434	0.027	0.143	521	533	599
FML 106a	0.185	0.030	0.040	1.259	0.443	0.035	0.183	496	514	587
FML 107a	0.191	0.035	0.049	1.249	0.445	0.034	0.183	511	526	594
FML 110	0.176	0.058	0.040	0.653	0.605	0.061	0.136	582	726	717
FML 113a	0.228	0.075	0.033	1.553	0.392	0.036	0.158	513	515	587
FML 116b	0.206	0.060	0.038	0.860	0.538	0.049	-0.145	581	676	689

*G-A Goldman and Albee (1977)
F-S Ferry and Spear (1977)
T A. B. Thompson (1976)

because K_D is largely insensitive to pressure (Albee, 1965). Temperatures for garnet–biotite pairs are also calculated with the calibrations of Ferry and Spear (1977) and of A. B. Thompson (1976) for comparison. The results are tabulated in Table 2, and temperatures calculated by the Goldman–Albee calibration correspond well to those calculated by the Ferry–Spear experimental calibration, except for three samples collected from the kyanite zone. Temperatures calculated with the A. B. Thompson calibration are in excess of the other two by 75–100°C. The high-grade pairs CP 435c, FML 110, and FML 116b show better correspondence in temperatures calculated from Ferry–Spear and Thompson. Comparison to experimental data and the correspondence between temperatures calculated by Goldman–Albee and Ferry–Spear for garnet- and staurolite-grade samples suggest that these may be realistic values. Similarly, temperatures calculated from Thompson for kyanite–sillimanite-grade samples seem more appropriate. The suggested temperature in the garnet-grade Indian Pass area is 470–500°C, at the staurolite isograd 500–530°C, and in the high-grade Monarch Canyon area 600–700°C.

The pressure during metamorphism is difficult to estimate for most mineral assemblages. Estimates based on the probable amount of overburden are unsatisfactory because the Paleozoic section exposed to the north (Reynolds, 1974) and to the south (McAllister, 1974) amounts to 6.2 km and 7.8 km respectively. The thickness of the Mesozoic cover at the presumed time of metamorphism (Cretaceous) is unknown, but if the thickness was comparable to that estimated in the Panamints, perhaps 3 km may be added. A generous estimate of 12 km of cover suggests lithostatic pressures on the order of 4 kbar, but the mineral assemblages suggest that pressures may have been approximately 1.5 to 2.0 times this amount.

In the high-grade rocks, the coexistence of garnet + plagioclase + kyanite + quartz allows the calculation of pressure, given the temperature. Ghent (1975, 1976) suggested the use of the divariant reaction

$$3 \text{ anorthite} = \text{grossular} + \text{kyanite} + \text{quartz}$$

as a potential geobarometer. The equilibrium constant is given by

$$0 = -\frac{3272}{T} - 8.3969 - \frac{0.3448(P-1)}{T} + \log a_{gros}^{gar} - 3 \log a_{an}^{plag}$$

(Ghent, 1976). The activity of anorthite in plagioclase is $\gamma_{an}^{plag} X_{an}^{plag}$, where $\gamma_{an}^{plag} = 1.28$ for sodic plagioclase (Orville, 1972). The activity of grossular in gar-

Table 3. Garnet–plagioclase–kyanite geobarometer and muscovite–plagioclase–kyanite geothermometer

SAMPLE	TEMP. °C	X^{plag}_{An}	X^{gar}_{gross}	$\ln \gamma_{gross}$	P bars	X^{plag}_{ab}	X^{mica}_{Na}	$\log \gamma^{mica}_{Na}$	f_{H_2O}	a_{H_2O}
CP 435c	538	0.265	0.050	0.560	6109	0.735	0.096	0.884	1639	0.478
	604			0.518	7239			0.842	4838	0.857
	645			0.495	7941			0.818	8761	1.153
FML 113a	513	0.157	0.033	0.599	6064	0.843	0.285	0.651	761	0.254
	515			0.597	6099			0.650	789	0.250
	587			0.547	7400			0.616	2629	0.457
FML 116b	581	0.157	0.038	0.545	7692	0.843	0.168	0.779	2998	0.486
	676			0.491	9408			0.732	11585	0.968
	689			0.484	9643			0.726	13653	1.050

net is given by $(\gamma^{gar}_{gros} X^{gar}_{gros})^3$, assuming random mixing in the three 8-fold sites; γ^{gar}_{gros} is estimated by assuming a regular symmetric solution model for the binary solution grossular–almandine, which gives (Ghent, 1975):

$$\ln \gamma^{gar}_{gros} = \frac{(1 - X^{gar}_{gross})^2}{RT} W$$

W, the regular symmetric solution parameter, derived from the excess free energy of mixing determined by Ganguly and Kennedy (1974), is estimated to be +1000 cal/mole.

Pressures were calculated from three samples from the kyanite zone for each temperature calculated by the K_D for coexisting garnet and biotite. The results are shown in Table 3, and show pressures from 6100 to nearly 10,000 bars. The estimated temperature range of 600°–700°C suggests the reasonable pressure range of 7200–9600 bars for the high-grade terrane in the Funeral Mountains. The large uncertainty in the temperature gives a tremendous uncertainty in pressure. Despite the great uncertainty, the results calculated for the kyanite zone samples are consistent with the experimental work of Ganguly (1972) and Richardson (1968) for the breakdown of staurolite.

The results of calculation of a_{H_2O} from the three kyanite-zone samples by the multi-variant reaction

$$\text{paragonite} + \text{quartz} = \text{albite} + \text{kyanite} = H_2O$$

(see Ghent, 1975) are inconclusive. Values (Table 3) ranging from 0.250 to essentially 1.0 may be derived from the estimated *P–T* pairs. The majority of the rocks are pelitic or quartzitic, whereas carbonate rocks are restricted to the high-grade regions; the fluid phase was probably rich in H_2O.

The mineral assemblages in pelitic schists from the Funeral Mountains preserve a nearly complete record of the facies series in a Barrovian metamorphic terrane. The compositions of the minerals suggest that during metamorphism the Funeral Mountains were buried to depths of approximately 20 km and that dP/dT in the highest-grade area was ~10 bar/°C (~30°C/km). This gradient is steep compared to gradients in the regional metamorphic terranes adjacent to the Mesozoic batholitic belt (*e.g.* the Panamint Mountains record a gradient of ~ 5 bar/°C; Labotka, 1980), and the Funeral Mountains are one of the few localities in the Cordillera that comprise an extensive kyanite-bearing terrane. This window through the higher, unmetamorphosed structural levels in the western Great Basin indicates that an extensive regional-metamorphism terrane every bit as complex and petrologically interesting as terranes in other orogenic belts underlies the North American Cordillera.

Acknowledgments

This work presents some of the results from my Ph.D. thesis supervised by Arden L. Albee, whose encouragement and criticism is appreciated. The study was supported by grants from the NSF (EAR75-03416A03 to A. L. Albee) and the Geological Society of America. I thank D. Rumble for his review of the manuscript.

References

Albee, A. L. (1965) Phase equilibria in three assemblages of kyanite-zone pelitic schists, Lincoln Mountain Quadrangle, central Vermont. *J. Petrol., 6*, 246–301.

——— (1968) Metamorphic zones in northern Vermont. In E-an Zen, W. S. White, J. B. Hadley and J. B. Thompson, Eds., *Studies of Appalachian Geology: Northern and Maritime*, p. 329–342. Wiley-Interscience, New York.

——— (1972) Metamorphism of pelitic schists: reaction relations of chloritoid and staurolite. *Geol. Soc. Am. Bull., 83*, 3249–3268.

——— and L. Ray (1970) Correction factors for electron probe microanalysis of silicates, oxides, carbonates, phosphates, and sulfates. *Anal. Chem., 42*, 1408–1414.

Bence, A. E. and A. L. Albee (1968) Empirical correction factors for the electron microanalysis of silicates and oxides. *J. Geol., 76*, 382–403.

Bird, G. W. and J. J. Fawcett (1973) Stability relations of Mg-chlorite–muscovite and quartz between 5 and 10 kb water pressure. *J. Petrol., 14*, 415–428.

Champion, D. E., A. L. Albee and A. A. Chodos (1975) Reproducibility and operator bias in a computer controlled system for quantitative electron microprobe analysis. *Proc. Tenth Annual Microbeam Analysis Soc. Conf.*, 55A–55F.

Chatterjee, N. D. (1972) The upper stability limit of the assemblage paragonite + quartz and its natural occurrences. *Contrib. Mineral. Petrol., 34*, 288–303.

——— and W. Johannes (1974) Thermal stability and standard thermochemical properties of synthetic $2M_1$-muscovite $KAl_2(AlSi_3O_{10}(OH)_2)$. *Contrib. Mineral. Petrol., 48*, 89–114.

Ferry, J. M. and F. S. Spear (1977) Experimental calibration of the partitioning of Fe and Mg between biotite and garnet (abstr.). *Geol. Soc. Am. Abstracts with Programs, 9*, 974.

Ganguly, J. (1972) Staurolite stability and related parageneses: theory, experiments, and applications. *J. Petrol., 13*, 335–365.

——— and G. C. Kennedy (1974) The energetics of natural garnet solid solution I. Mixing of the aluminosilicate end-members. *Contrib. Mineral. Petrol., 48*, 137–148.

Ghent, E. D. (1975) Temperature, pressure, and mixed volatile equilibria attending metamorphism of staurolite–kyanite-bearing assemblages, Esplanade Range, British Columbia. *Geol. Soc. Am. Bull., 86*, 1654–1660.

——— (1976) Plagioclase–garnet–Al_2SiO_5–quartz: a potential geobarometer–geothermometer. *Am. Mineral., 61*, 710–714.

Goldman, D. S. and A. L. Albee (1977) Correlation of Mg/Fe partitioning between garnet and biotite with $^{18}O/^{16}O$ partitioning between quartz and magnetite. *Am. J. Sci., 277*, 750–767.

Harte, B. (1975) Determination of a pelitic petrogenetic grid for the eastern Scottish Dalradian. *Carnegie Inst. Wash. Year Book, 74*, 438–446.

Holdaway, M. J. (1971) Stability of andalusite and the aluminum silicate phase diagram. *Am. J. Sci., 271*, 97–131.

Hollister, L. S. (1966) Garnet zoning: an interpretation based on the Rayleigh fractionation model. *Science, 154*, 1647–1651.

Hoschek, G. (1969) The stability of staurolite and chloritoid and their significance in metamorphism of pelitic rocks. *Contrib. Mineral. Petrol., 22*, 208–232.

Kerrick, D. M. (1968) Experiments on the upper stability limit of pyrophyllite at 1.8 kilobars and 3.9 kilobars water pressure. *Am. J. Sci., 266*, 204–214.

Labotka, T. C. (1980) Late Mesozoic regional metamorphism in Death Valley, California: petrology of the low-pressure, Panamint metamorphic terrane. *J. Petrol.*, in press.

———, A. L. Albee, M. A. Lanphere and S. D. McDowell (1980) Stratigraphy, structure, and metamorphism in the central Panamint Mountains, Death Valley area, California. *Geol. Soc. Am. Bull., 91*, in press.

McAllister, J. F. (1974) Geologic maps and sections of a strip from Pyramid Peak to the southeast end of the Funeral Mountains, Ryan Quadrangle, California. In *Guidebook: Death Valley Region, California and Nevada*, p. 81–82. Shoshone, Death Valley Publishing Company.

Orville, P. M. (1972) Plagioclase cation exchange equilibria with aqueous chloride solution: results at 700°C and 2000 bars in the presence of quartz. *Am. J. Sci., 272*, 234–272.

Reynolds, M. W. (1974) Geology of the Grapevine Mountains, Death Valley, California: a summary. In *Guidebook: Death Valley Region, California and Nevada*, p. 91–97. Shoshone, Death Valley Publishing Company.

Richardson, S. W. (1968) Staurolite stability in a part of the system Fe–Al–Si–O–H. *J. Petrol., 9*, 467–488.

Thompson, A. B. (1976) Mineral reactions in pelitic rocks: I. Prediction of *P–T–X* (Fe–Mg) phase relations. II. Calculation of some *P–T–X* (Fe–Mg) phase relations. *Am. J. Sci., 276*, 401–454.

———, P. T. Lyttle and J. B. Thompson (1977) Mineral relations and A–Na–K and A–F–M facies types in the Gassetts Schist, Vermont. *Am. J. Sci., 277*, 1124–1151.

Thompson, J. B. (1957) The graphical analysis of mineral assemblages in pelitic schists. *Am. Mineral., 42*, 842–858.

Troxel, B. W. and L. A. Wright (1968) Precambrian stratigraphy of the Funeral Mountains, Death Valley, California (abstr.). *Geol. Soc. Am. Spec. Pap., 121*, 574–575.

Tuttle, O. F. and N. L. Bowen (1958) Origin of granite in light of experimental studies in the system $NaAlSi_3O_8$-$KAlSi_3O_8$–SiO_2–H_2O. *Geol. Soc. Am. Mem. 74.*

Wasserburg, G. J., G. W. Wetherill and L. A. Wright (1959) Ages in the Precambrian terrain of Death Valley, California. *J. Geol., 67*, 702–708.

Manuscript received, August 8, 1979;
accepted for publication, December 19, 1979.